Published in final edited form as:
Stem Cells. 2009 March ; 27(3): 489–497. doi:10.1634/stemcells.2008-0855.

Evidence for transcriptional regulation of the glucose-6-phosphate transporter by HIF-1α: Targeting G6PT with mumbaistatin analogs in hypoxic mesenchymal stromal cells

Simon Lord-Dufour[1], **Ian B. Copland**[2], **Louis-Charles Levros Jr**[3], **Martin Post**[4], **Abhirup Das**[5], **Chaitan Khosla**[5], **Jacques Galipeau**[2], **Eric Rassart**[3], and **Borhane Annabi**[1,*]

[1]Laboratoire d'Oncologie Moléculaire, Département de Chimie, Centre BIOMED, Université du Québec à Montréal, Quebec, Canada

[2]Department of Medicine, Lady Davis Institute for Medical Research, Montreal, Quebec, Canada

[3]Laboratoire de Biologie Moléculaire, Département des Sciences Biologiques, Université du Québec à Montréal, Quebec, Canada

[4]Lung Biology Research Program, The Hospital for Sick Children Research Institute, Toronto, Ontario, Canada

[5]Departments of Chemistry, Chemical Engineering and Biochemistry, Stanford University, Stanford California, USA

Abstract

Mesenchymal stromal cells (MSC) markers are expressed on brain tumor-initiating cells involved in the development of hypoxic glioblastoma. Given that MSC can survive hypoxia and that the glucose-6-phosphate transporter (G6PT) provides metabolic control that contributes to MSC mobilization and survival, we investigated the effects of low oxygen (1.2% O_2) exposure on G6PT gene expression. We found that MSC significantly expressed G6PT and the glucose-6-phosphatase catalytic subunit β (G6PC-3), while expression of the glucose-6-phosphatase catalytic subunit α (G6PC) and the islet-specific glucose-6-phosphatase catalytic subunit-related protein (G6PC-2) gene expression was low to undetectable. Analysis of the G6PT promoter sequence revealed potential binding sites for the hypoxia inducible factor-1 (HIF-1) α and for the aryl hydrocarbon receptor (AhR) and its dimerization partner, the AhR nuclear translocator (ARNT) AhR:ARNT. In agreement with this, hypoxia and the hypoxia mimetic cobalt chloride induced the expression of G6PT, vascular endothelial growth factor (VEGF) and HIF-1α. Gene silencing of HIF-1α prevented G6PT and VEGF induction in hypoxic MSC while generation of cells stably expressing HIF-1α resulted in increased endogenous G6PT gene expression. A semi-synthetic analog of the polyketide mumbaistatin, a potent G6PT inhibitor, specifically reduced MSC-HIF-1αcell survival. Collectively, our data suggest that G6PT may account for the metabolic

*To whom correspondence and reprint requests should be directed, Laboratoire d'Oncologie Moléculaire, Université du Québec à Montréal, C.P. 8888, Succ. Centre-ville, Montréal, Québec, CANADA, H3C 3P8, Phone : (514) 987-3000 ext. 7610, Fax : (514) 987-0246, E-mail : annabi.borhane@uqam.ca.

Author contribution: Lord-Dufour : Collection and assembly of data, data analysis, manuscript writing
Copland : Collection and assembly of data, manuscript writing
Levros Jr : Collection and assembly of data
Post : Collection and assembly of data
Das : Collection and assembly of data
Khosla : Data analysis, manuscript writing
Galipeau : Collection of data, Data analysis, manuscript writing
Rassart : Data analysis, manuscript writing
Annabi : Conception and design, data analysis, manuscript writing, financial support

flexibility that enables MSC to survive under conditions characterized by hypoxia and could be specifically targeted within developing tumors.

Keywords

Mesenchymal stromal cells; hypoxia inducible factor-1 alpha; glucose-6-phosphate transporter; stem cell migration; brain tumor

INTRODUCTION

Molecular markers associated with mesenchymal stromal cells (MSC) are thought to characterize the brain tumor-initiating cells involved in the development of glioblastoma, the most common and aggressive primary brain cancer (1). Given that glioblastoma are also highly hypoxic tumors (2), these findings suggest that a subset of primary glioblastomas may derive from transformed stem cells containing MSC-like properties and retaining partial phenotypic aspects of the MSC nature within the tumors' hypoxic environment. Bone marrow-derived MSC are a population of pluripotent adherent cells residing within the bone marrow microenvironment that can differentiate into many mesenchymal phenotypes (3,4). Interestingly, the recruitment of MSC by experimental vascularizing tumors has resulted in the incorporation of MSC within the tumor architecture (5,6), which implies that these cells must respond to tumor-derived growth factor cues (7,8). More importantly, their potential contribution to tumor development also implies that MSC must adapt to the low oxygen environment and nutrient deprivation that characterizes hypoxic tumors.

MSC were recently demonstrated also to have the capacity to survive under conditions of ischemia and to resist hypoxic culture conditions (9). Furthermore, resistance of MSC to inhibition of mitochondrial respiration also indicates that MSC can survive in the absence of oxygen using both anaerobic ATP production and increased glycolysis (9). The control of glycolysis and of gluconeogenesis occurs primarily at the level of the interconversion of fructose-6-phosphate and fructose-1,6-bisphosphate under the action of phosphofructokinase-1 (PFK-1) and fructose-1,6-bisphosphatase (10). Increased glycolysis is essential for the survival and spread of cancer cells in low oxygen environment. Under these conditions, the key step in controlling the glycolytic rate involves PFK-1, whose activation is controlled by the hypoxia-inducible factor-1 (HIF-1) complex (11). HIF-1 is a transcription factor that is induced during the adaptation of tumour cells to hypoxia, activating the transcription of genes which, in turn, regulate several biological processes including angiogenesis, cell proliferation and survival, glucose metabolism, pH regulation and migration (12). HIF-1α, the oxygen-sensitive subunit of HIF-1, was shown to induce the recruitment of bone marrow-derived vascular modulatory cells and trigger processes involved in tumor angiogenesis and invasion (13). It also regulates homing of marrow-derived progenitor cells to injured tissue (14). Whether alternate intracellular metabolic systems, such as the glucose-6-phosphatase (G6Pase) system, would enable MSC to survive under conditions of hypoxic stress and whether these systems would be regulated by the HIF-1 complex are currently unknown.

Recently, impaired chemotaxis was reported in bone marrow cells isolated from a G6PT deficient ($G6PT^{-/-}$) mouse (15,16). In agreement with those reports, we have demonstrated that G6PT can regulate cell migration (17) as well as MSC chemotaxis and survival (18). In fact, since its discovery, G6PT has been shown to be responsible for G6P transport from the cytosol to the lumen of the endoplasmic reticulum (ER), therefore performing the rate-limiting step for G6P hydrolysis into glucose and inorganic phosphate by the G6Pase system. G6PT has been shown to integrate and regulate many metabolic functions such as

glycemia, lipidemia, uricemia, and lactic acidemia (19). More importantly, its activity cannot be substituted as G6PT deficiencies lead to glycogen storage disease (GSD) type Ib characterized not only by disturbed glucose homeostasis but by severe myeloid dysfunctions (19). Beside MSC, G6PT is believed to play a role in neutrophil chemotaxis and calcium flux control (20–23), and in U87 glioma cell survival (24,25). In turn, G6PT gene expression is regulated in response to adaptive metabolic changes involving glucose, insulin and cyclic AMP (26). In this study, we investigated whether transcription of G6PT could be further regulated under the control of hypoxia-responsive elements, and to what extent G6PT could promote MSC survival under hypoxic conditions.

MATERIALS AND METHODS

Materials

Sodium dodecylsulfate (SDS) and bovine serum albumin (BSA) were purchased from Sigma (Oakville, ON). Cell culture media were obtained from Life Technologies (Burlington, ON). Electrophoresis reagents were purchased from Bio-Rad (Mississauga, ON). The enhanced chemiluminescence (ECL) reagents were from Amersham Pharmacia Biotech (Baie d'Urfé, QC). Micro bicinchoninic acid protein assay reagents were from Pierce (Rockford, IL). The polyclonal antibodies against HIF-1α and PARP were from Chemicon (Temecula, CA). The polyclonal antibodies against phospho-Akt, phospho-Erk and GAPDH were purchased from Cell Signaling (Danvers, MA).

Cell culture and experimental hypoxic conditions

Bone marrow-derived mesenchymal stromal cells (MSC) were isolated from the whole femur and tibia bone marrow of C57BL/6 female mice; cells were cultured and characterized as previously described (27). Analysis by flow cytometry, performed at passage 14, revealed that MSC expressed CD44 yet were negative for CD45, CD31, KDR/flk1 (VEGF-R2), flt-4 (VEGF-R3) and Tie2 (angiopoietin receptor) (data not shown). Cells were cultured in serum-free DMEM during drug treatment in order to approximate the pathophysiological conditions of low growth factors and nutrient availability such as that found within the hypoxic environment of developing tumors. Hypoxic conditions were attained by incubation of confluent cells in an anaerobic box. The oxygen was maintained at 1% by a compact gas oxygen controller Proox model 110 (Reming Bioinstruments Co., Redfield, NY) with a residual gas mixture composed of 94% N_2 and 5% CO_2.

cDNA construct generation and transduction of the MSC-HIF-1α

The human full-length HIF-1α cDNA construct was generously provided by Dr. Semenza (Johns Hopkins University, Baltimore, MD, USA), and was used as a template for generating an HIF-1α mutant which lacked its oxygen-dependent degradation domain ($ODD_{401–603}$). The deletion mutant (HIF-1α ΔODD) was constructed by overlap extension using PCR. The deletion was confirmed by DNA sequencing, and the 1.95 kb HIF-1α ΔODD cDNA was subcloned into pcDNA3.1. For generation of retroviral particles, the HIF-1α ΔODD construct was digested out of the pcDNA3.1 vector using BamHI and HpaI restriction enzymes and subcloned into the multiple cloning site of the bicistronic retrovector pIRES-GFP. 293-GP2 viral packaging cells were transfected with either the HIF-1α ΔODD-pIRES-GFP or null-pIRES-GFP plasmids and the viral supernant was collected at 48 and 72 hours post-transfection. MSC were subjected to 8 rounds of viral transduction. Following viral transduction each GFP(+)MSC (AP2-MSC) and HIF-1α-ΔODD-GFP(+) MSC population were each subjected to high speed cell sorting (BD FacsAria) to obtain polyclonal pooled clones of retrovirally-transfected MSC that were 100% GFP(+) and similar in regards to GFP signal intensity.

Immunoblotting procedures

Nuclear extracts from MSC or MSC-HIF-1α were isolated using the NE-PER Nuclear and cytoplasmic extraction kit (Pierce, Rockford, IL) and proteins separated by SDS–polyacrylamide gel electrophoresis (PAGE). After electrophoresis, proteins were electrotransferred to polyvinylidene difluoride membranes which were then blocked for 1 hr at room temperature with 5% non-fat dry milk in Tris-buffered saline (150 mM NaCl, 20 mM Tris–HCl, pH 7.5) containing 0.3% Tween-20 (TBST). Membranes were further washed in TBST and incubated with the anti-HIF-1α primary antibody (1/1,000 dilution) in TBST containing 3% BSA, followed by a 1 hr incubation with horseradish peroxidase-conjugated anti-rabbit IgG in TBST containing 5 % non-fat dry milk. Immunoreactive material was visualized by enhanced chemiluminescence (Amersham Biosciences, Baie d'Urfée, QC).

Cell migration assay

MSC or MSC-HIF-1α were trypsinized and seeded at 10^5 cells on 0.15% gelatin/PBS precoated Transwells (Corning/Costar; Acton, MA; 8-μm pore size) assembled in 24-well Boyden chambers which were filled with 600 μl of serum-free media. Cell migration was allowed to proceed for 6 hours at 37°C in 5% CO_2. Non-migrating cells that remained on the upper side of the Transwell filter were carefully removed with cotton swabs. Cells that had migrated to the lower side of the filters were fixed with 3.7% formaldehyde and stained with 0.1% crystal violet/20% MeOH and counted. The migration was quantified by analyzing at least ten random fields per filter for each independent experiment using the computer-assisted imaging software Northern Eclipse 6.0 (Empix Imaging Inc., Mississauga, ON).

Total RNA isolation, cDNA synthesis and real-time quantitative RT-PCR

Total RNA was extracted from MSC monolayers using TRIzol reagent (Life Technologies, Gaithersburg, MD). For cDNA synthesis, 1 μg of total RNA was reverse-transcribed into cDNA using a high capacity cDNA reverse transcription kit (Applied Biosystems, Foster City, CA). cDNA was stored at −80°C prior to PCR. Gene expression was quantified by real-time quantitative PCR using iQ SYBR Green Supermix (BIO-RAD, Hercules, CA). DNA amplification was carried out using an Icycler iQ5 (BIO-RAD, Hercules, CA) and product detection was performed by measuring binding of the fluorescent dye SYBR Green I to double-stranded DNA. All the QuantiTect primer sets were provided by QIAGEN (Valencia, CA): Mm_Hif1a_1_SG QT01039542, Mm_Slc37a4_1_SG QT00124411, Mm_G6pc_1_SG (NM_008061) QT00114625, Mm_G6pc2_1_SG (NM_021331) QT00139461, Mm_G6pc3_1_SG (NM_175935) QT00104748. The relative quantities of target gene mRNA against an internal control, 18S ribosomal RNA, were measured by following a ΔC_T method employing an amplification plot (fluorescence signal *vs*. cycle number). The difference (ΔC_T) between the mean values in the triplicate samples of target gene and those of 18S ribosomal RNA were calculated by iQ5 Optical System Software version 2.0 (BIO-RAD, Hercules, CA) and the relative quantified value (RQV) was expressed as $2^{-\Delta C_T}$.

Semi-quantitative RT-PCR analysis

One microgram of total RNA was used for first strand cDNA synthesis followed by specific gene product amplification with the One-Step RT-PCR kit (Invitrogen). Primers used were the same as for the qRT-PCR and were all derived from mouse sequences. GAPDH cDNA amplification was used as an internal house-keeping gene control. PCR conditions were optimized so that the gene products were examined at the exponential phase of their amplification and the products were resolved on 2.2% agarose gels containing 1 μg/ml ethidium bromide.

Transfection method and RNA interference

MSC were transiently transfected with 20 μM siRNA against HIF-1α (Mm_Hif1a_1 HP siRNA, SI00193011) using HiPerFect (QIAGEN, CA). HIF-1α-specific gene knockdown was evaluated by qRT-PCR as described above. Small interfering RNA against HIF-1α and mismatch siRNA were synthesized by QIAGEN and annealed to form duplexes.

Morphological analysis of apoptotic and necrotic cells

To visualize nuclear morphology and chromatin condensation by fluorescence microscopy (18), cells were pretreated for 18 h with chlorogenic acid (CHL), the mumbaistatin analog (AD4-015), or with their respective vehicle (Ethanol or DMSO). Cells were stained with 0.06 mg/ml Hoechst (33258, blue fluorescence) for apoptotic cells or with 50 μg/ml propidium iodide (red fluorescence) for necrotic cells. Observations were made by fluorescence microscopy (Carl Zeiss Ltd, Montreal, QC, Canada) and photographs were taken with a digital camera (camera 3CCD, Sony DXC-950P, Empix Imaging Inc, Mississauga, ON). Images were analyzed by Northern Eclipse software. A minimum of 600 cells was counted per dish.

Electrophoretic Mobility Shift Assays

Fifty ng of sense oligonucleotide was 5'- end-labeled with T4 polynucleotide kinase and [γ-^{32}P]ATP and annealed with 200 ng of the complementary oligonucleotide. Nuclear extracts from growing MSC-HIF-1α were prepared according to the method of Dignam *et al.* (28). Nuclear extracts were analyzed by gel shift assays as described previously (29). Thirty μg of nuclear extract were added to 0.8 ng of the labeled double-stranded oligonucleotide, and, after a 20-min incubation at 11 room temperature, the mixture was run on a 6% acrylamide, non-denaturing gel in 0.5× TBE, at 150 V for 90 min. The dried gels were autoradiographed on Kodak X-Omat films. For competition assays, a 25-fold excess (20 ng) of cold double-stranded oligonucleotide was added before addition of the nuclear extract. The sense strand sequences of the oligonucleotides used are: HIF-1α, CCG AGG CTA CGT GCG GCT TCT CTC G; NSC (unrelated sequence), CCA AAC AGG ATA TCT GTA ATA AGC AG.

RESULTS

Murine MSC strongly express the G6PT component of the glucose-6-phosphatase system

In order to confirm expression of the G6PT component in MSC, semi-quantitative RT-PCR was performed using total RNA extracted from mouse MSC, mouse liver, and from mouse pancreas. Measurement of the other 3 components of the G6Pase system : the glucose-6-phosphatase catalytic subunit α (G6PC), the islet-specific glucose-6-phosphatase catalytic subunit-related protein (G6PC-2), and the glucose-6-phosphatase catalytic subunit β (G6PC-3) was also performed. Compared to liver or pancreas, MSC significantly expressed G6PT. In contrast, G6PC and G6PC-3 were expressed at low to undetectable levels in MSC and pancreas in comparison to liver. As expected, G6PC-2 gene expression was clearly detected in pancreas, while its expression was very low in MSC and undetectable in liver (Fig.1). GAPDH served as an internal loading control and remained constant. In contrast to hepatocytes, which predominantly utilize a-ketoacids as fuel, MSC may presumably heavily depend on G6P for their energy needs.

Cobalt chloride-induced chemical hypoxia and hypoxic culture conditions regulate G6PT gene expression

MSC were serum-starved and cultured under hypoxic conditions (18 hours under 1.2% O_2) or treated with cobalt chloride ($CoCl_2$), a condition known to mimic hypoxic culture

conditions. Total RNA was extracted and qRT-PCR performed as described in the Methods section. We found that hypoxia significantly induced HIF-1α transcript levels in agreement with previous reports (30,31), a mechanism that could involve Egr-1 transcriptional regulation of HIF-1α (31). In support to that assumption, Egr-1 increase at the protein level during hypoxia was documented by us previously in MSC (32). Moreover, VEGF and G6PT gene expression were also induced, while G6PC-3 and membrane type-1 matrix metalloproteinase (MT1-MMP) remained unchanged (Fig.2a, black bars). Treatment of the cells with $CoCl_2$ also triggered VEGF and G6PT gene expression, while expression of HIF-1α, G6PC-3 and MT1-MMP remained unaffected (Fig.2a, grey bars). One can conclude that, in the case of $CoCl_2$ treatments, it's not the induction of HIF-1α but the potential blockade of HIF-1α degradation via prolyl hydroxylation and subsequent interaction with the VHL factor and targeting to proteasomal degradation that may additionally be in play in G6PT regulation. These observations prompted us to analyze the murine G6PT gene promoter sequence for the presence of any hypoxia responsive elements (HRE) that could regulate its expression under low oxygen tension. We examined a DNA sequence of 1207 bp upstream of the ATG start codon (NCBI source NM_008063.2) and located on mouse chromosome 9 at location 44,205,182-44,211,045 (Fig.2b). A search for putative transcription factor binding sites was performed with PROMO 3.0 (http://alggen.lsi.upc.es/) using version 8.3 of the TRANSFAC database. A TATA box as well as several previously reported binding sites were found within the first 200 bp upstream of the ATG and included HNF1, HNF3, and C/EBP binding sites (33). The core consensus sequence of HRE that we searched for was (A/G)CGT(G/C)C and is denoted by asterisks (*) (34). We found one potential binding site for HIF-1, and two for AhR:Arnt (Fig.2b, boxed). This suggests that possible G6PT transcriptional regulation may occur in MSC upon hypoxic culture conditions. Whether HIF-1α was involved in such G6PT gene regulation was next explored.

Gene silencing of HIF-1a antagonizes the effects of hypoxia on G6PT gene expression

We used gene silencing strategies to down-regulate HIF-1α gene expression and to assess its specific contribution to G6PT gene regulation under hypoxic culture conditions. MSC were transiently transfected with scrambled sequences (Mock) or with HIF-1α siRNA as described in the Methods section. Cells were then cultured under normal or hypoxic culture conditions, total RNA was extracted and qRT-PCR was used to assess HIF-1α, VEGF, and MT1-MMP gene expression. We found that HIF-1α gene expression was efficiently reduced in siHIF-1α-transfected cells (Fig.3a, black bars). VEGF gene expression was also reduced in siHIF-1a-transfected cells, and the increase in VEGF expression under hypoxia was reduced by ~58% (Fig.3a, black bars). MT1-MMP gene expression in siHIF-1α-transfected cells remained unaffected. G6PT gene expression was also measured in Mock-transfected (Fig.3b, open circles) and in siHIF-1α-(closed circles) transfected cells that were subsequently cultured under hypoxic conditions (Fig.3b). While G6PT gene expression was transiently increased by hypoxia with a maximum expression at 10 hours in Mock cells, those cells where HIF-1α gene expression was abrogated were unable to increase G6PT gene expression. Consequently, expression of HIF-1α is required for G6PT transcriptional regulation upon hypoxia. Since silencing experiments of HIF-1α by themselves do not allow one to prove that HIF-1α directly binds to the G6PT promoter, approaches such as chromatin immunoprecipitation assays will be needed. Although the cascade of events may still be indirect, we are confident to have experimentally demonstrated that HIF-1α is a crucial intermediate in the sequence of events that regulate G6PT gene expression.

Constitutive expression of an oxygen-dependent degradation domain HIF-1a mutant triggers G6PT gene expression

In order to recreate the hypoxic culture conditions that trigger HIF-1α expression in MSC, we generated a deletion mutant of HIF-1α (HIF-1α ΔODD) and stably transfected MSC as

described in the Methods section. We found that MSC constitutively and stably expressing HIF-1α ΔODD (MSCHIF-1α) exhibited an increased intrinsic ability to migrate (Fig.4a). Such increased migratory potential has been documented previously (32) and, although speculative, may potentially involve autocrine regulation through hypoxia-regulated growth factors expression. This may provide efficient mobilization and adaptative behaviour of MSC to oxygen deprived environment. When total RNA was extracted from MSC or MSC-HIF-1α, we found that HIF-1α, VEGF, MT1-MMP, and G6PT gene expression were significantly increased in MSC-HIF-1α cells (Fig.4b, black bars). In order to confirm that HIF-1α could potentially directly interact with HRE sequences found within the G6PT promoter, we isolated nuclear extracts from MSC-HIF-1α and showed that HIF-1α protein was indeed constitutively present within the nuclear fraction of MSC-HIF-1α while nuclear poly-(ADP-ribose) polymerase (PARP) expression remained constant (Fig.4c). Electrophoretic mobility assays was also performed in order to demonstrate that nuclear HIF-1α interacted with radiolabeled oligonucleotides (mHIF-1) containing the HIF-1α sequence found within the G6PT promoter. Incubation of the MSC-HIF-1α nuclear extracts with those probes resulted in the formation of 3 complexes termed A, B, and C (Fig.4d, column 1). Complexes B and C binding to the probe was strongly diminished upon competition with a 25-fold excess of a cold unrelated non-specific competitor (NSC), suggesting these were non-specific binding. In contrast, complex A remained intense (Fig. 4d, column 2) but completely disappeared with the same excess of the cold HIF-1α specific competitor (SC) or in the presence of an HIF-1α blocking antibody (Fig.4d, columns 3 and 4).

A small molecule G6PT inhibitor specifically triggers cell death in MSC constitutively expressing HIF-1α ΔODD

Specific targeting of hypoxic cells such as those found within a tumor microenvironment is a difficult task to achieve. Since we have found that hypoxic MSC express high levels of G6PT, we hypothesized that these cells would be sensitive to G6PT inhibitors. We used chlorogenic acid (CHL), a natural product with weak G6PT inhibitory activity (35) and a more potent semi-synthetic polyketide analog (AD4-015) of a different natural product mumbaistatin (36) (Fig.5a). Dose-response curves for G6PT inhibition by AD4-015 in both rat liver microsomal assays as well as hepatocyte assays were reported earlier (36). In the microsomal assay, the IC_{50} was 2.5 μM, while in the cell-based assay, inhibition was only observed at 10-fold higher concentrations, a feature that is constant with all known G6PT inhibitors and is presumably a reflection of target access (see discussion in reference 36). Because that cell-based assay more accurately reflects our own MSC assays, we used a concentration of 25 μM in the current assays. MSC and MSC-HIF-1α were thus treated with 100 μM CHL or 25 μM AD4-015, and cell death assessed. We found that increased Hoechst staining (apoptosis) as well as PI staining (necrosis) was observed in treated MSC-HIF-1α in comparison to MSC (Fig.5b). Cell death was not significantly induced by CHL, while AD4-015 triggered ~3-times more cell death in MSC-HIF-1α (Fig.5c). In support to the prosurvival phenotype ascribed to MSC-HIF, their basal levels of phospho-Akt and phospho-Erk protein expression were found increased when compared to MSC (Fig.5d). Treatment of the cells with AD4-015 was found to specifically downregulate phospho-Akt expression levels in MSC-HIF but not in MSC (Fig.5d) suggestive of targeted cell death induction in MSC-HIF. Altogether, these data suggest that small molecule inhibitors of G6PT may show selectivity in targeting hypoxic MSC.

DISCUSSION

Most commonly isolated from the bone marrow, MSC are multipotent adult stem cells with immunomodulatory effects and the ability to home to sites of injury. These properties,

clearly useful for therapeutic purposes, may however be used by cancer cells for their own ends. Indeed, as the importance of the microenvironment and stroma to the evolution and progression of solid tumors has been revealed over the past few years, MSC which are the progenitors of stromal cells and fibroblasts have been found to interact with cancer cells (37). In fact, the homing of MSC to tumors is thought to be the earliest phenomenon of MSC-cancer interactions, as was recently reported in a mouse model where injected human MSC could be found preferentially migrating to implanted human melanoma tumors (5). Subsequently, studies have shown MSC homing to tumors and even to sites of metastasis (38). Furthermore, cotransplantation of MSC with melanoma cells in mice enhanced tumor engraftment and growth (39). These data are in agreement with our own observations that vascular progenitors derived from bone marrow stromal cells are recruited by tumors both *in vivo* and *in vitro* (7). Collectively, the sum of this evidence, in line with the increased ability of MSC to migrate under an atmosphere of low oxygen as is seen in the tumor microenvironment (32), suggests that MSC are active participants in the development of solid tumors.

The expression of a number of glycolytic isozymes (*e.g.* PFK-L, ALD-A, ALD-C, PGK-1, ENO-1, and LDH-A) has already been found to be induced by hypoxia in a tissue-specific manner (40,41). Analysis of the *cis*-acting sequences of these genes has revealed that hypoxia-induced activation requires binding sites for HIF-1. All the above genes, together with G6PT, reflect the adaptative capacity of MSC to oxygen deprivation. Pharmacological targeting of G6PT functions, and hence inducing possible glucose deprivation conditions, should thus be deleterious to the hypoxic cell as denoted by our own data in Fig.5b and Fig. 5d where cell death was specifically triggered. In this report, we have undertaken a detailed study to delineate the role of G6PT that could link metabolic and survival adaptation to hypoxia in MSC. Through the generation of an MSC-HIF-1α stable cell line and through the use of siRNA gene silencing strategies, we also showed that HIF-1α is involved in the transcriptional regulation of G6PT. As a consequence, G6PT gene expression was increased by hypoxia supporting a prosurvival role for G6PT. In agreement with this observation, G6PT-deficient neutrophils isolated from GSD-Ib mice are characterized by increased rates of apoptosis (42), possibly consequent to increased expression of ER stress-related, glucose-regulated proteins and protein disulfide isomerase (43,44). These findings are thus in agreement with the ubiquitous expression and prosurvival functions of G6PT that were reported in glioma cells and in MSC (18,24). Investigation of whether increased G6PT functions could potentially affect the glycolytic phenotype and make hypoxic MSC gluconeogenic must also be considered in the metabolic adaptation phenotype to hypoxia.

Alternate G6PT roles, distinct from its classical involvement in the G6Pase system, include ATP-mediated calcium sequestration in the ER lumen (45), activity as a G6P receptor/sensor (46), and supplying G6P to a ubiquitously expressed luminal glucose-6-phosphate dehydrogenase (47). One or more of these functions may also be responsible for crucial prosurvival processes including tumor cell proliferation, cell cycle division and extracellular matrix degradation. In fact, the observed increases in MSC-HIF of ERK phosphorylation and AKT phosphorylation correlate with the high migratory and prosurvival phenotype observed. Our current study thus supports these functions of the ubiquitously expressed G6PT in non-gluconeogenic tissues. Furthermore, the luminal hexose-6-phosphate dehydrogenase also provides reducing equivalents needed for several important reductases that protect the ER against damage by reactive oxygen species. Lack of protection may result in premature cell death through apoptosis.

In light of the role of G6PT in MSC biology that has been highlighted by our results, selective interference with G6PT functions and/or expression may be an attractive therapeutic approach to metabolic control of cancer cell growth or in preventing circulating

cells from being recruited to contribute to tumor development. Indeed, gene silencing of G6PT has already been shown to suppress intracellular signaling that leads to calcium mobilization by sphingosine-1-phosphate (23), a potent bio-active lipid and inducer of MSC mobilization (27). Here, we further demonstrate that small molecule G6PT inhibitor AD4-015 can induce apoptosis and necrosis of hypoxic MSC (MSC-HIF-1α) and that show high sustained endogenous G6PT gene expression. Noteworthy, treatment of MSC under hypoxic conditions with AD4-015 did not result in any difference in cell death most probably because G6PT gene expression is transient, peaking at ~8 hours of hypoxia (Fig. 3b). We believe that our MSC-HIF-1α model better reflects the long term metabolic adaptation of the cells to hypoxia and highlights the specific contribution of HIF-1α on G6PT gene expression. Altogether, this may provide some rationale for a potentially new therapeutic action against hypoxic cells embedded within tumors.

Since studies have so far been limited to a few types of cancers, it is still unknown how MSC interact with other cancers, if at all. Whether the animal models used accurately reflect what actually occurs within the hypoxic tumor setting remains to be established, because most *in vivo* experiments use high numbers of exogenously introduced MSC, an unlikely scenario in the endogenous state. Still, exogenously delivered human MSC were reported to specifically localize to human gliomas after intravascular delivery (6), which raises the possibility that endogenous MSC may be recruited into hypoxic gliomas during tumorigenesis and may contribute to the physiological growth of brain tumors *in situ*. Preliminary data from our own work also provides data demonstrating high G6PT expression within experimental hypoxic brain tumors (data not shown). Furthermore, tumor-derived MSC were recently isolated and characterized as CD133(−) cells, indicating that they were distinct from classic CD133(+) glioma cancer stem cells. These CD133(−)-MSC were more commonly isolated from high grade tumors than from low grade gliomas, supporting the hypothesis that tumor-derived MSC are involved in glioma progression from low to high grade (48). Accordingly, extremely low CD133(−) glioblastomas were found to show mesenchymal subclass-like gene expression profile, which has the worst clinical outcome (49).

In conclusion, our study reveals a potential metabolic adaptation of MSC to hypoxic conditions that enables MSC to survive under conditions characterized by low oxygen levels and glucose deprivation, such as is found within developing tumors. Such metabolic flexibility may, in part, be accounted for by the prosurvival functions of G6PT that would allow these MSC to contribute to tumor development. More importantly, hypoxic MSC that contribute to tumor development may also be selectively targeted by small molecules G6PT inhibitors such as the semisynthetic polyketide derivative AD4-015, modeled after the natural product mumbaistatin.

Acknowledgments

BA holds a Canada Research Chair in Molecular Oncology from the Canadian Institutes of Health Research (CIHR). This study was funded by a grant from the United States National Institutes of Health to CK (CA 77248), and by a grant of the Natural Sciences and Engineering Research Council of Canada (NSERC) to BA.

REFERENCES

1. Tso CL, Shintaku P, Chen J, et al. Primary glioblastomas express mesenchymal stem-like properties. Mol Cancer Res. 2006; 4:607–619. [PubMed: 16966431]
2. Kaur B, Khwaja FW, Severson EA, et al. Hypoxia and the hypoxia-inducible-factor pathway in glioma growth and angiogenesis. Neuro Oncol. 2005; 7:134–153. [PubMed: 15831232]
3. Prockop DJ. Marrow stromal cells as stem cells for nonhematopoietic tissues. Science. 1997; 276:71–74. [PubMed: 9082988]

4. Horwitz EM, Le Blanc K, Dominici M, et al. The International Society for Cellular Therapy. Clarification of the nomenclature for MSC: The International Society for Cellular Therapy position statement. Cytotherapy. 2005; 7:393–395. [PubMed: 16236628]
5. Studeny M, Marini FC, Champlin RE, et al. Bone marrow-derived mesenchymal stem cells as vehicles for interferon-beta delivery into tumors. Cancer Res. 2002; 62:3603–3608. [PubMed: 12097260]
6. Nakamizo A, Marini F, Amano T, et al. Human bone marrow-derived mesenchymal stem cells in the treatment of gliomas. Cancer Res. 2005; 65:3307–3318. Erratum in: Cancer Res. 2006; 66:5975. [PubMed: 15833864]
7. Annabi B, Naud E, Lee YT, et al. Vascular progenitors derived from murine bone marrow stromal cells are regulated by fibroblast growth factor and are avidly recruited by vascularizing tumors. J Cell Biochem. 2004; 91:1146–1158. [PubMed: 15048870]
8. Birnbaum T, Roider J, Schankin CJ, et al. Malignant gliomas actively recruit bone marrow stromal cells by secreting angiogenic cytokines. J Neurooncol. 2007; 83:241–247. [PubMed: 17570034]
9. Mylotte LA, Duffy AM, Murphy M, et al. Metabolic flexibility permits MSC survival in an ischemic environment. Stem Cells. 2008; 26:1325–1336. [PubMed: 18308942]
10. Hers HG. Mechanisms of blood glucose homeostasis. J Inherit Metab Dis. 1990; 13:395–410. [PubMed: 2122108]
11. Bartrons R, Caro J. Hypoxia, glucose metabolism and the Warburg's effect. J Bioenerg Biomembr. 2007; 39:223–229. [PubMed: 17661163]
12. Patiar S, Harris AL. Role of hypoxia-inducible factor-1alpha as a cancer therapy target. Endocr Relat Cancer. 2006; 13 Suppl 1:S61–S75. [PubMed: 17259560]
13. Du R, Lu KV, Petritsch C, et al. HIF1alpha induces the recruitment of bone marrow-derived vascular modulatory cells to regulate tumor angiogenesis and invasion. Cancer Cell. 2008; 13:206–220. [PubMed: 18328425]
14. Ceradini DJ, Gurtner GC. Homing to hypoxia: HIF-1 as a mediator of progenitor cell recruitment to injured tissue. Trends Cardiovasc Med. 2005; 15:57–63. [PubMed: 15885571]
15. Kim SY, Nguyen AD, Gao JL, et al. Bone marrow-derived cells require a functional glucose 6-phosphate transporter for normal myeloid functions. J Biol Chem. 2006; 281:28794–28801. [PubMed: 16891306]
16. Yiu WH, Pan CJ, Allamarvdasht M, et al. Glucose-6-phosphate transporter gene therapy corrects metabolic and myeloid abnormalities in glycogen storage disease type Ib mice. Gene Ther. 2007; 14:219–226. [PubMed: 17006547]
17. Belkaid A, Currie JC, Desgagnés J, et al. The chemopreventive properties of chlorogenic acid reveal a potential new role for the microsomal glucose-6-phosphate translocase in brain tumor progression. Cancer Cell Int. 2006; 6:7. [PubMed: 16566826]
18. Currie JC, Fortier S, Sina A, et al. MT1-MMP down-regulates the glucose 6-phosphate transporter expression in marrow stromal cells: a molecular link between pro-MMP-2 activation, chemotaxis, and cell survival. J Biol Chem. 2007; 282:8142–8149. [PubMed: 17229722]
19. Chou JY, Matern D, Mansfield BC, et al. Type I glycogen storage diseases: disorders of the glucose-6-phosphatase complex. Curr Mol Med. 2002; 2:121–143. [PubMed: 11949931]
20. Chen LY, Shieh JJ, Lin B, et al. Impaired glucose homeostasis, neutrophil trafficking and function in mice lacking the glucose-6-phosphate transporter. Hum Mol Genet. 2003; 12:2547–2558. [PubMed: 12925567]
21. Leuzzi R, Bánhegyi G, Kardon T, et al. Inhibition of microsomal glucose-6-phosphate transport in human neutrophils results in apoptosis: a potential explanation for neutrophil dysfunction in glycogen storage disease type 1b. Blood. 2003; 101:2381–2387. [PubMed: 12424192]
22. Cheung YY, Kim SY, Yiu WH, et al. Impaired neutrophil activity and increased susceptibility to bacterial infection in mice lacking glucose-6-phosphatase-beta. J Clin Invest. 2007; 117:784–793. [PubMed: 17318259]
23. Fortier S, Labelle D, Sina A, et al. Silencing of the MT1-MMP/ G6PT axis suppresses calcium mobilization by sphingosine-1-phosphate in glioblastoma cells. FEBS Lett. 2008; 582:799–804. [PubMed: 18267120]

24. Belkaid A, Copland IB, Massillon D, et al. Silencing of the human microsomal glucose-6-phosphate translocase induces glioma cell death: potential new anticancer target for curcumin. FEBS Lett. 2006; 580:3746–3752. [PubMed: 16777101]
25. Belkaid A, Fortier S, Cao J, et al. Necrosis induction in glioblastoma cells reveals a new "bioswitch" function for the MT1-MMP/G6PT signaling axis in proMMP-2 activation versus cell death decision. Neoplasia. 2007; 9:332–340. [PubMed: 17460777]
26. van de Werve G, Lange A, Newgard C, et al. New lessons in the regulation of glucose metabolism taught by the glucose 6-phosphatase system. Eur J Biochem. 2000; 267:1533–1549. [PubMed: 10712583]
27. Meriane M, Duhamel S, Lejeune L, et al. Cooperation of matrix metalloproteinases with the RhoA/Rho kinase and mitogen-activated protein kinase kinase-1/extracellular signal-regulated kinase signaling pathways is required for the sphingosine-1-phosphate-induced mobilization of marrow-derived stromal cells. Stem Cells. 2006; 24:2557–2565. [PubMed: 16931773]
28. Dignam JD, Lebovitz RM, Roeder RG. Accurate transcription initiation by RNA polymerase II in a soluble extract from isolated mammalian nuclei. Nucleic Acids Res. 1983; 11:1475–1489. [PubMed: 6828386]
29. Benson BA, Butler YX, Ackerman M, et al. A kinase/phosphatase system involving the protooncogene Lck is necessary for inducible modulation of Sob 1 during T cell activation. Cell Immunol. 1996; 170:245–250. [PubMed: 8660824]
30. Belaiba RS, Bonello S, Zahringer C, et al. Hypoxia up-regulates hypoxia-inducible factor-1alpha transcription by involving phosphatidylinositol 3-kinase and nuclear factor kappaB in pulmonary artery smooth muscle cells. Mol Biol Cell. 2007; 18:4691–4697. [PubMed: 17898080]
31. Sperandio S, Fortin J, Sasik R, et al. The transcription factor Egr1 regulates the HIF-1alpha gene during hypoxia. Mol Carcinog. 2008 (in press).
32. Annabi B, Lee YT, Turcotte S, et al. Hypoxia promotes murine bone-marrow-derived stromal cell migration and tube formation. Stem Cells. 2003; 21:337–347. [PubMed: 12743328]
33. Hiraiwa H, Pan CJ, Lin B, et al. A molecular link between the common phenotypes of type 1 glycogen storage disease and HNF1alpha-null mice. J Biol Chem. 2001; 276:7963–7967. [PubMed: 11121425]
34. Kimura H, Weisz A, Ogura T, et al. Identification of hypoxia-inducible factor 1 ancillary sequence and its function in vascular endothelial growth factor gene induction by hypoxia and nitric oxide. J. Biol. Chem. 2001; 276:2292–2298. [PubMed: 11056166]
35. Hemmerle H, Burger HJ, Below P, et al. Chlorogenic acid and synthetic chlorogenic acid derivatives: novel inhibitors of hepatic glucose-6-phosphate translocase. J Med Chem. 1997; 40:137–145. [PubMed: 9003513]
36. Lee TS, Das A, Khosla C. Structure-activity relationships of semisynthetic mumbaistatin analogs. Bioorg Med Chem. 2007; 15:5207–5218. [PubMed: 17524653]
37. Yen BL, Yen ML. Mesenchymal Stem Cells and Cancer — for Better or for Worse? Journal of Cancer Molecules. 2008; 4:5–9.
38. Dwyer RM, Potter-Beirne SM, Harrington KA, et al. Monocyte chemotactic protein-1 secreted by primary breast tumors stimulates migration of mesenchymal stem cells. Clin Cancer Res. 2007; 13:5020–5027. [PubMed: 17785552]
39. Djouad F, Plence P, Bony C, et al. Immunosuppressive effect of mesenchymal stem cells favors tumor growth in allogeneic animals. Blood. 2003; 102:3837–3844. [PubMed: 12881305]
40. Semenza GL, Roth PH, Fang HM, et al. Transcriptional regulation of genes encoding glycolytic enzymes by hypoxia-inducible factor 1. J. Biol. Chem. 1994; 269:23757–23763. [PubMed: 8089148]
41. Ebert BL, Gleadle JM, O'rourke JF, et al. Isoenzyme-specific regulation of genes involved in energy metabolism by hypoxia: similarities with the regulation of erythropoietin. Biochem. J. 1996; 313:809–814. [PubMed: 8611159]
42. Kuijpers TW, Maianski NA, Tool AT, et al. Apoptotic neutrophils in the circulation of patients with glycogen storage disease type 1b (GSD1b). Blood. 2003; 101:5021–5024. [PubMed: 12576310]

43. Lee AS. The glucose-regulated proteins: stress induction and clinical applications. Trends Biochem Sci. 2001; 26:504–510. [PubMed: 11504627]
44. Schröder M, Kaufman RJ. The mammalian unfolded protein response. Annu Rev Biochem. 2005; 74:739–789. [PubMed: 15952902]
45. Chen PY, Csutora P, Veyna-Burke NA, et al. Glucose-6-phosphate and Ca2+ sequestration are mutually enhanced in microsomes from liver, brain, and heart. Diabetes. 1998; 47:874–881. [PubMed: 9604862]
46. Hiraiwa H, Pan CJ, Lin B, et al. Inactivation of the glucose 6-phosphate transporter causes glycogen storage disease type 1b. J Biol Chem. 1999; 274:5532–5536. [PubMed: 10026167]
47. van Schaftingen E, Gerin I. The glucose-6-phosphatase system. Biochem J. 2002; 362:513–532. [PubMed: 11879177]
48. Lang, FF.; Amano, T.; Hata, N., et al. Tumor-derived mesenchymal stem cells in human gliomas: Isolation and biological effects; Proceedings from the 2008 Annual AACR meeting; San Diego, USA.
49. Joo, KM.; Kim, SY.; Kim, MH., et al. CD133-negative glioblastoma cancer stem cells represent the ‘mesenchymal’ subclass of glioblastoma; Proceedings from the 2008 Annual AACR meeting; San Diego, USA.
50. Messeguer X, Escudero R, Farré D, et al. PROMO: detection of known transcription regulatory elements using species-tailored searches. Bioinformatics. 2002; 18:333–334. [PubMed: 11847087]
51. Farré D, Roset R, Huerta M, et al. Identification of patterns in biological sequences at the ALGGEN server: PROMO and MALGEN. Nucleic Acids Res. 2003; 31:3651–3653. [PubMed: 12824386]

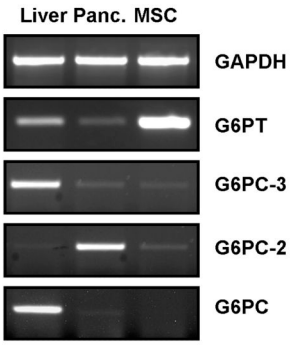

Fig.1. Murine MSC strongly express the G6PT component of the glucose-6-phosphatase system

Total RNA was extracted from mouse MSC, mouse liver, and from mouse pancreas as described in the Methods section. cDNA synthesis and semi-quantitative RT-PCR were performed to assess gene expression of the glucose-6-phosphate transporter (G6PT), the glucose-6-phosphatase catalytic subunit α (G6PC), the islet-specific glucose-6-phosphatase catalytic subunit-related protein (G6PC-2), and the glucose-6-phosphatase catalytic subunit β (G6PC-3).

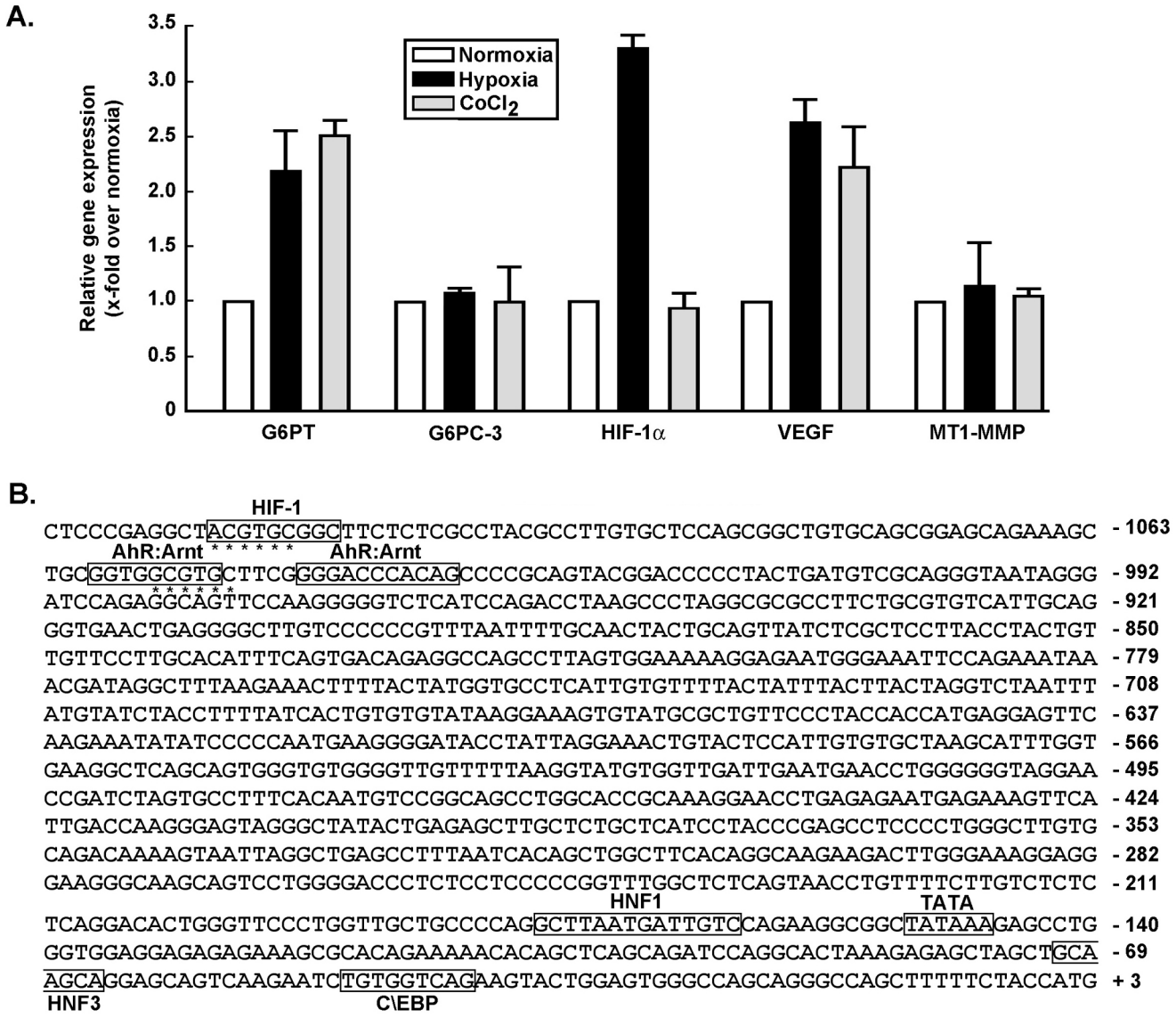

Fig.2. Cobalt chloride-induced chemical hypoxia and hypoxic culture conditions regulate G6PT gene expression

(A) Sub-confluent MSC were serum-starved and cultured under normoxic (5% CO_2 and 95% air; white box), or hypoxic (1% O_2, 5% CO_2, and 94% N_2; black box) conditions, or treated with 100 μM $CoCl_2$ (grey box) for 18 hours. Total RNA was extracted and qRT-PCR performed in order to assess the G6PT, G6PC-3 HIF-1α, VEGF, and MT1-MMP gene expression levels. (B) A 1133 bp sequence upstream of the ATG coding sequence of the murine G6PT gene promoter sequence was analyzed (NCBI source NM_008063.2), and located on mouse chromosome 9 at location 44,205,182-44,211,045. The core consensus sequence of the hypoxia responsive elements (A_G)CGT(G_C)C is denoted by asterisks (*, 50,51). Sequences of a TATA box (−152/−147) and potential binding sites for HIF-1 (−1122/−1114), AhR:Arnt (−1059/−1051 and −1045/−1035), HNF1 (−177/−164), HNF3 (−71/−65), and C/EBP (−48/−40) are boxed.

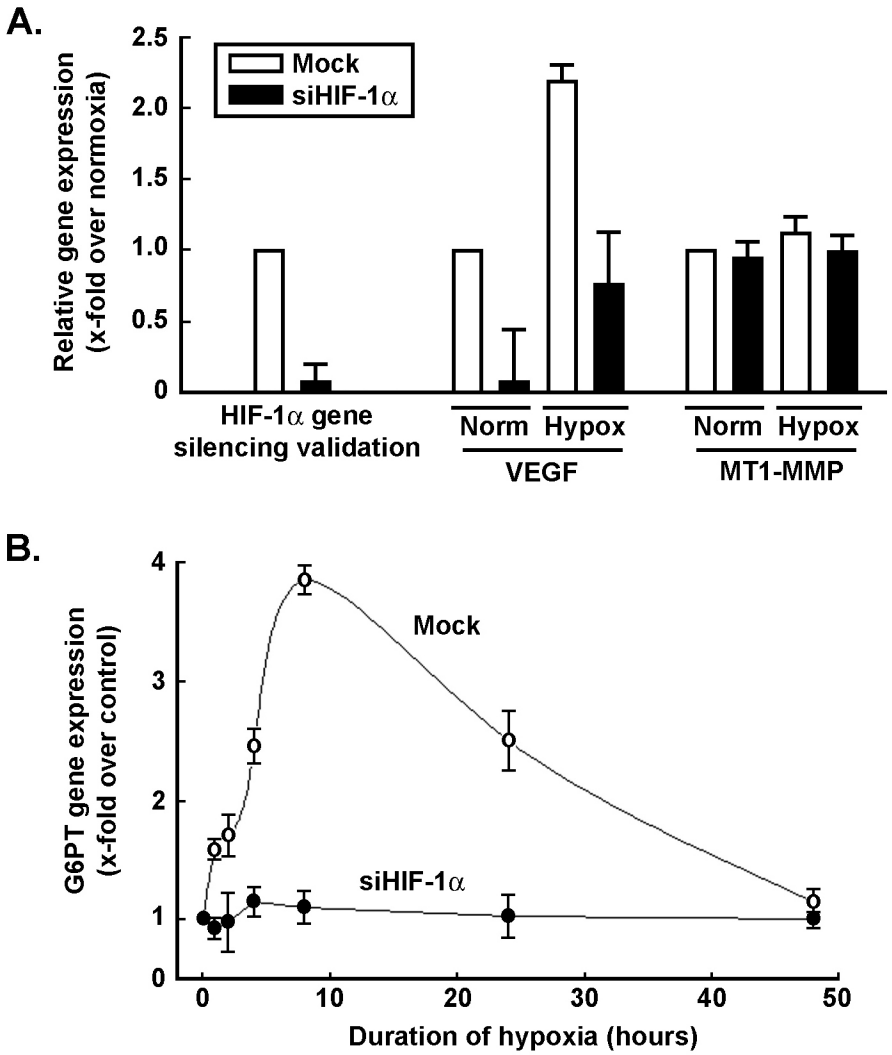

Fig.3. Gene silencing of HIF-1α antagonizes the effects of hypoxia on G6PT gene expression

(A) MSC were transiently transfected with scrambled sequences (Mock, white bars) or HIF-1α siRNA (black bars) as described in the Methods section. Cells were then cultured under normal or hypoxic culture conditions, total RNA was extracted and qRT-PCR was used to assess HIF-1α, VEGF, and MT1-MMP gene expression as described in Fig.2. (B) G6PT gene expression was assessed by qRT-PCR in Mock-transfected (open circles) and in siHIF-1α-(closed circles) transfected cells that were subsequently cultured under hypoxic conditions.

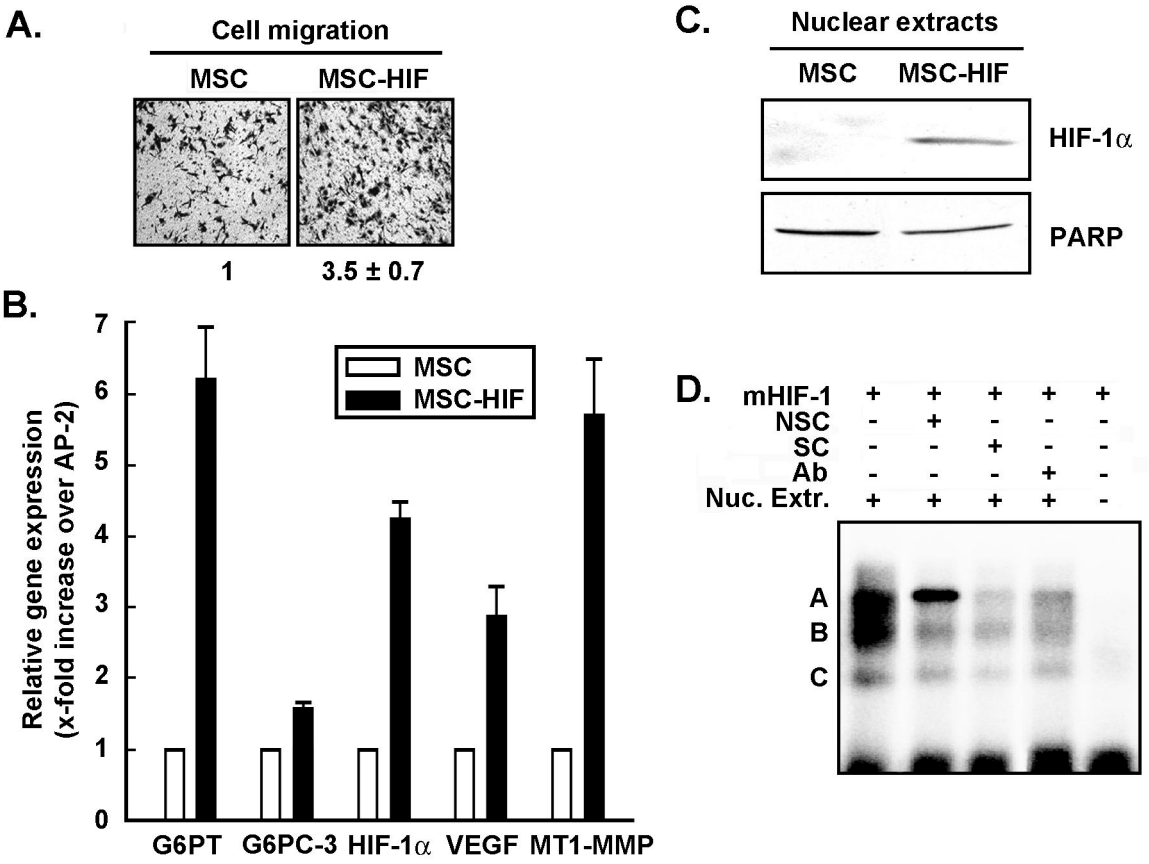

Fig.4. Constitutive expression of an oxygen-dependent degradation domain HIF-1α mutant triggers G6PT gene expression

(A) Basal migration of MSC and MSC stably expressing a deletion mutant of HIF-1α (HIF-1α ΔODD, MSC-HIF) was performed as described in the Methods section. (B) Total RNA was extracted from MSC (white bars) and MSC-HIF (black bars), and qRT-PCR performed to assess the gene expression levels of G6PT, G6PC-3, VEGF, HIF-1α, and MT1-MMP. (C) Nuclear extracts were islolated from MSC and MSC-HIF and Westernblotting performed to detect nuclear HIF-1α or nuclear poly-(ADP-ribose) polymerase (PARP) expression. (D) Electrophoretic mobility assays were performed as described in the Methods section using nuclear extracts (Nuc. Extr.) isolated from MSC-HIF. NSC, cold unrelated non-specific competitor; SC, cold HIF-1α specific competitor; Ab, HIF-1α (1 μg) blocking antibody.

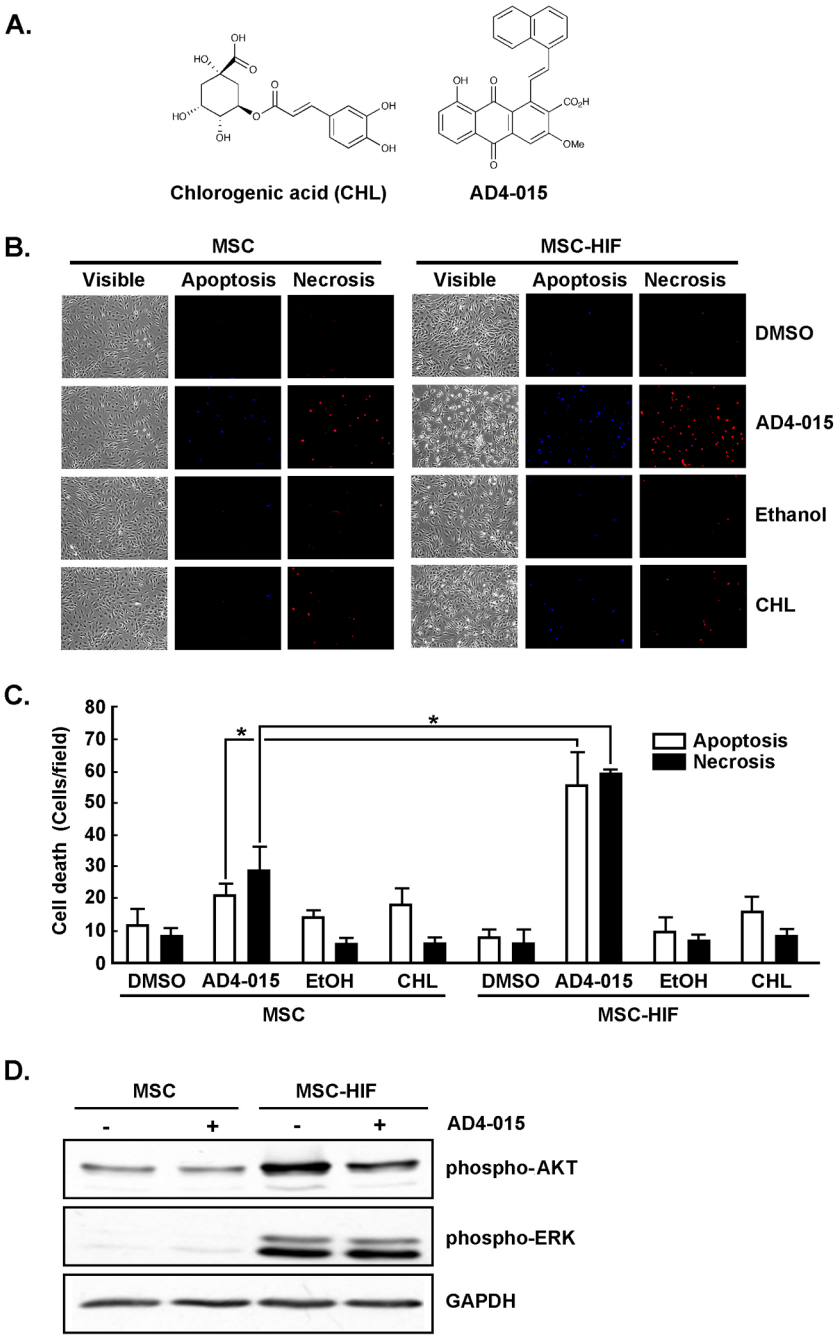

Fig.5. The mumbaistatin analog and potent G6PT inhibitor AD4-015 specifically triggers cell death in MSC constitutively expressing HIF-1α ΔODD

(A) Chemical structures of chlorogenic acid (CHL) and mumbaistatin analog (AD4-015). (B) MSC or MSC-HIF were cultured under normoxic conditions then treated for 18 hrs with 25 μM AD4-015 (or respective DMSO vehicle), or with 100 μM CHL (or respective EtOH vehicle). Hoechst (apoptosis) and propidium iodide (necrosis/late apoptosis) cell labelling was then performed and visualised using fluorescence microscopy. (C) Quantification was performed by visual counting. The mean of 4 fields from 3 independent experiments is shown. Probability values of less than 0.05 were considered significant, and an asterisk (*) identifies such significance. (D) MSC and MSC-HIF were treated with AD4-015 as in (B)

and lysates isolated. SDS-PAGE followed by immunodetection of phospho-Erk, phospho-Akt, or GAPDH was performed as described in the Methods section.